Effect of lumbar support on vibration transmission of a car seat with occupant exposed to fore-and-aft whole-body vibration

Hui Zhou[1], Yi Qiu[1] and Roberto Lot[2]
Institute of Sound and Vibration Research[1]
Engineering Sciences[2]
University of Southampton
Southampton SO17 1BJ
United Kingdom

Abstract:

Modern car seats are often equipped with adjustable lumbar supports for reducing fatigue and improving ride comfort in different driving conditions. Studies on the effect of lumbar support on seat dynamic performance and ride comfort are not often seen. This experimental study was designed to investigate how lumbar support affects static and dynamic characteristics of the driver seat of a sport utility vehicle. The load-deflection curves of the backrest cushion of the car seat were measured in three extra lumbar support conditions (regarded as "No", "Half" and "Full" lumbar supports). The acceleration transmissibilities to the backrest and to the seat pan in the fore-and-aft direction with different lumbar support conditions were measured with 8 male subjects exposed to random fore-and-aft vibration from 1 to 30 Hz with three magnitudes (0.25, 0.5, 1.0 ms^{-2} r.m.s), using a Multi-Axis Simulation Table. It was found that the lumbar area of the backrest became stiffer with increased extra lumbar support. The peak at the resonance of the acceleration transmissibility from the seat base to the backrest decreased, while that in the transmissibility from the seat base to the seat pan increased, when increasing the lumbar support. The softening effect was also apparent with increasing vibration magnitude. It is anticipated that changing the lumbar support will affect the static comfort of the seat and also the vibration transmission through the seat to occupant.

1. Introduction

A modern car seat is often designed in terms of ergonomics and the comfort expectations of the driver or passenger (Kolich, 2003). It should not only provide static comfort but also function as a vibration isolator in different driving conditions. Various adjustable functionalities, such as seat position adjusters, backrest angle controller and lumbar support adjuster, are integrated in the seat to meet various customer needs so as to improve ride comfort and reduce fatigue. This paper is concerned with the effect of lumbar support of the backrest on the static and dynamic performance of a car seat.

Static performance of vehicle seats, often examined with the cushion hardness (characterised by load-deflection curves) and pressure distribution, has been reported to affect the overall comfort in static conditions (e.g. Kamijo *et al*., 1982; Ebe and Griffin, 2000; Ebe and Griffin, 2001). The extra lumbar support of the backrest of a car seat was found to significantly reduce the pressure on discs and muscles of the seated human body (Andersson *et al*., 1974). A study about the relationship between seat pressure distribution and subjective responses suggested that higher pressure ratios at the upper and lower back could effectively improve the sitting comfort (Kyung and Nussbaum, 2008). A passive lumbar motion system of the seat in an earthmoving equipment was found to help control the low back discomfort and reduce fatigue of the driver (Viswanathan *et al*., 2006). Zhang *et al*. (2013) conducted an experimental study on hardness distribution of a car seat and found the hardness varied over the

Presented at the 51st United Kingdom Conference on Human Responses to Vibration, held at Institute of Naval Medicine, Gosport, PO12 2DL, England, 14 - 16 September 2016

surface of the seat pan. However, studies concerned with the hardness distribution of seat backrest with the different lumbar support conditions are rarely reported.

Seat backrest is suggested to be treated as an important discomfort source especially for vibration exposure in the fore-and-aft direction (BS 6841: 1987; ISO 2631-1: 1997). Qiu and Griffin (2003) investigated acceleration transmissibilities to the backrest and to the seat pan in the fore-and-aft direction for a car seat using both laboratory simulation and field measurement. Three resonances at about 5, 28 and 48 Hz in the fore-and-aft transmissibilities from the seat base to the backrest were declared, and the peak transmissibility at the primary resonance was found to decrease with increasing the vibration magnitude. Later studies also found that the primary resonance frequency and the associated peak transmissibility from seat base to backrest in the fore-and-aft direction decreased with increasing the vibration magnitude (Jalil and Griffin, 2007a; Zhang *et al.*, 2015). Jalil and Griffin (2007b) studied the fore-and-aft transmissibility to backrests of a car seat and a rigid seat with foam when the backrest inclination angle was changed from vertical (90°) to 105° backwards in exposure of random fore-and-aft vibration. It was reported in their study that increasing the backrest inclination resulted in the increase of both the resonance frequency and the associated peak transmissibility for the car seat but little change for the rigid backrest with foam. The measurement position on the backrest was also reported to significantly affect the assessment of dynamic performance of the backrest: the transmissibility was greatest at the middle of the backrest near the lumbar support area during fore-and-aft vibration (Jalil and Griffin, 2007a). Although adjustable lumbar support has been commonly used in modern car seats, there were very few studies about the effect of lumbar support on the vibration transmission through the seat to occupant.

The objective of this paper is to investigate the effect of lumbar support of the backrest on seat static performance and whole-body vibration transmission to a car seat in fore-and-aft direction. It is anticipated that the presence of a lumbar support will affect the hardness distribution of the backrest and alter vibration transmission to the backrest and to the seat pan in the fore-and-aft direction.

2. Method

2.1 Apparatus

2.1.1 Test seat

The test seat was the front driver seat of a Sport Utility Vehicle provided by a project partner. The seat pan, backrest and headrest with shaped foams fully encased within fabric covers were supported on metal frames. The backrest contained a control rotating knob which could be used to adjust the lumbar support condition by the seated person. Other accessories including height and seat track position adjustment motors with moulded cases attached to the seat frame.

2.1.2 IRB 6620 Industrial Robot

An economical six-axis ABB industrial robot (Type: IRB 6620) was used in the quasi-static compression test to obtain load-deflection curves for the backrest of the test seat. The built-in position sensors of the robot can accurately measure three-dimensional positions of an object with a resolution of 0.03 mm. An aluminium (Type: EN-AW 5083) indenter head in hemisphere-shape of 50 mm diameter with adequate

rigidity, strength and smoothness surface was used in the measurements. Emergency stops are available in both the portable controller of the robot and the central control computer for the safety of the experimenters.

2.1.3 Multi-Axial Simulation Table

The vibration transmission in fore-and-aft direction through the test seat with different lumbar support conditions was measured with an MTS hexapod multi-axial simulation table (MAST) system which is driven by six servohydraulic actuators. The MAST table is capable of linear displacements of ±130 mm in the fore-and-aft direction, ±115 mm in the lateral direction and ± 145 mm in the vertical direction. The lightweight square table with dimensions of 2.2 m X 2.17 m consists of a flat steel plate with hollow cores and webbed construction. The simulator has a nominally flat frequency response from 0.8 Hz to 150 Hz, controlled by MTS RPC Pro software.

2.1.4 Transducers and data acquisition

For the hardness distribution test, a static force sensor (ATI Omega 160) mounted between the robot and the indenter head, was used to acquire the translational forces in the vertical direction. The maximum detectable force is 2500 N in the vertical direction with a resolution of 0.25 N.

For the seat transmissibility test, two piezo-electrical designed Metra's Seat pads (type: KB103SVD), met the specification set out in ISO 10326-1 (1992), were adopted to measure accelerations at the seat pan and the backrest. The Seat pads had an operating range of ± 50 g, working frequencies 1-1000 Hz and a voltage sensitivity of (100 ± 5%) mV/g for three directions. Motions of the simulation table were measured using a tri-axial MEMS accelerometer (S/N: C005562). It had an operating range of ± 50 g and a sensitivity of approximately 200 mV/g. Acceleration signals were recorded through the SoMat EHLS eDAQ system and sampled at 512 samples per second with a cut-off frequency of 100 Hz.

2.2 Test procedure

The experiments were conducted in a laboratory of a project collaborator, which was approved by the Automotive Engineering Research Institute of the China Automotive Technology and Research Centre (CATARC).

Before the test, the angles of the seat pan, backrest and headrest were adjusted and kept unchanged during the test: seat pan was reclined by 10° to the horizontal, backrest was reclined by 21° to the vertical, and headrest was reclined by 15° to the vertical.

The air temperature during the tests was in a range from 20 ℃ to 24 ℃.

2.2.1 Hardness distribution test

The hardness distribution of the backrest cushion was obtained by measuring the load-deflection curves at some predefined points over the backrest. A similar test procedure used in studying static characteristics of a car seat (Zhang *et al.,* 2013) was adopted. The measurement points along the centreline of the backrest were marked as points A to H from the headrest towards the seat pan (Figure 1). Point F regarded as the base point, was 100 mm above the H-point of the seat along the vertical

direction. Through point F, drawn a horizontal crossline from left to right of the backrest along which four extra measurement points marked 1 to 4 were defined (Figure 1). The spacing of each two points along the centreline and crossline of the backrest was about 50 mm.

The hardness distribution was tested with three backrest lumbar support conditions: no extra lumbar support (marked as “No”) corresponding to the knob start position (the subject was in a normal contact position with the backrest), half extra lumbar support (marked as “Half”) corresponding to the knob rotated clockwise one and a half circles, and full extra lumbar support (marked as “Full”) corresponding to the knob rotated to the maximum position (three circles). The load-deflection curves of the backrest at all marked points were measured with the three lumbar support conditions, respectively.

The seat was secured on the ground under the six-axis robot (Figure 2). Firstly, a preload of 2.5 N was applied at the position of each point by controlling the robot vertically downwards to the point. Then the force and displacement transducers were zeroed. Following that, the load was applied continuously until the force reached 150 N and then unload to force zero. During the test, the loading and unloading speed was set at a rate of 2.5 mm/s and the loads and displacements were acquired.

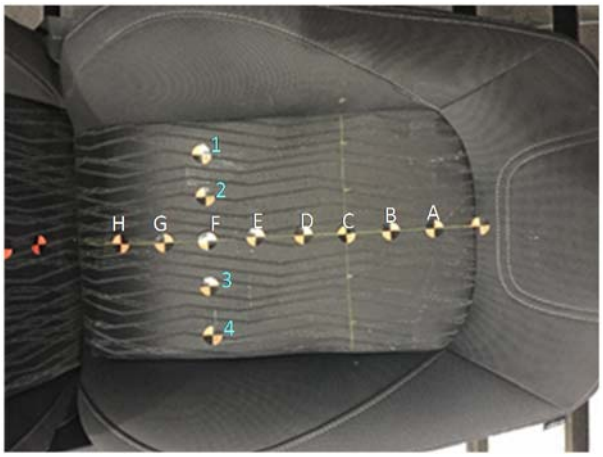

Figure 1 Measurement points on backrest

Figure 2 Hardness distribution (load-deflection curve) test of the backrest

2.2.2 Seat transmissibility test

To measure vibration transmission of the seat in the fore-and-aft direction, the test seat was mounted at the centre of the multi-axis simulation table. As shown in Figure 3, two Metra’s Seat pads taped to the cushions. The seat pad at the seat pan was positioned such that the pad was beneath the ischial tuberosities of the test subject. The seat pad at the backrest was centrally located 290 mm above the surface of the relaxed seat cushion and care was taken to ensure the subject was in a good contact with the pad. The tri-axial accelerometer was attached to the simulation table at the centre of the seat fixture beneath the test seat.

The excitation to the seat was random fore-and-aft vibration frequency ranged from 1 to 30 Hz with three magnitudes 0.25, 0.5 and 1.0 ms^{-2} r.m.s., each lasting 120 s. Eight healthy male volunteers aged between 22 and 28 years, weighted between 50 and 91 kg participated in the experiment (median age 26 years, median weight 69.8 kg, median height 175 cm). The subjects were recruited from the staff of the project collaborator. During the test, subjects wore a loose lap-belt and placed their hands on their

laps, with their back comfortably contacting the backrest and the feet supporting on the platform (Figure 4). Emergency stop buttons were situated within a reachable distance for both the experimenter and the subjects.

Figure 3 Positions of the transducers on the platform, seat pan and backrest

Figure 4 The test seat with a human subject

2.3 Data analysis

The transmissibility of the seat, $H(f)$, was calculated with the acceleration measured at the seat base (input) and the acceleration measured at the seat pan or backrest (output), using the cross-spectral density (CSD) method:

$$H(f) = \frac{G_{io}(f)}{G_{ii}(f)} \tag{1}$$

with the coherency $\gamma_{io}(f)$ calculated from:

$$\gamma_{io}^2(f) = \frac{|G_{io}(f)|^2}{G_{ii}(f)G_{oo}(f)} \tag{2}$$

where $G_{io}(f)$ is the cross-spectral density of the input and output accelerations, $G_{ii}(f)$ is the power spectral density of the input acceleration, and $G_{oo}(f)$ is the power spectral density of the output acceleration. The coherency $\gamma_{io}(f)$ is in the range of 0 to 1.

The transmissibility $H(f)$ contains both modulus and phase information:

$$H(f) = \sqrt{(\mathrm{Re}[H(f)])^2 + (\mathrm{Im}[H(f)])^2} \tag{3}$$

$$\varphi(f) = \tan^{-1}\left[\frac{\mathrm{Im}[H(f)]}{\mathrm{Re}[H(f)]}\right] \tag{4}$$

The transmissibilities were calculated with frequency resolution 0.25 Hz, using *HVLab* signal processing toolbox in Matlab R2014a.

3. Results

3.1 Load-deflection curve

The load-deflection curves of the base point F (close to the lumbar position) tested in three lumbar support conditions are shown in Figure 5. The curves show a hysteresis pattern and with the same deformation, the reaction force was greater when loading than when unloading. Similar hysteresis loops were observed in the load-deflection curves of other measurement points. Besides, for point F, the backrest cushion became stiffer when the lumbar support was increased from “No” to “Full” positions.

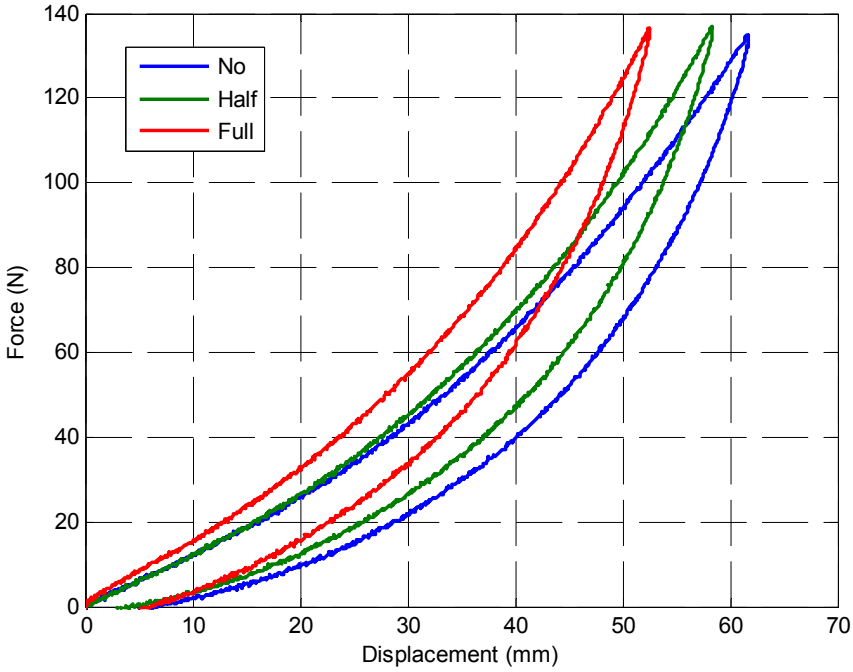

Figure 5 Load-deflection curves of backrest point F in three lumbar support conditions

In order to check the hardness distribution of the backrest cushion, the loading forces of points A to H at the deformation equal to 30 mm were extracted and plotted vs. position in Figure 6, for the three lumbar support conditions. There is a considerable increase of the loading force from “No” to “Full” lumbar support conditions for points D to H, while a slight increase of the force was observed between “Half” and “No” conditions at the same measurement points. With the same deformation of 30 mm, the increase of the loading force becomes apparent with increasing the distance between the measurement point and the headrest, except for point E which was relatively soft. It is also worth noting that there is no obvious difference in the loading forces at the test points A, B and C for the three lumbar support conditions.

The loading forces extracted from the points 1-4 and F along the crossline when the deformation equal to 30 mm are shown in Figure 7. The load-deflection curves were almost symmetric with respect to the centreline of the backrest. Similar to most points distributed in the centreline of the backrest, the loading force increased with increasing the lumbar support. The force did not change much between “Half” and

“No” lumbar support conditions for the all five points, while apparent increases of the force were observed when the lumbar support was adjusted to the “Full” position.

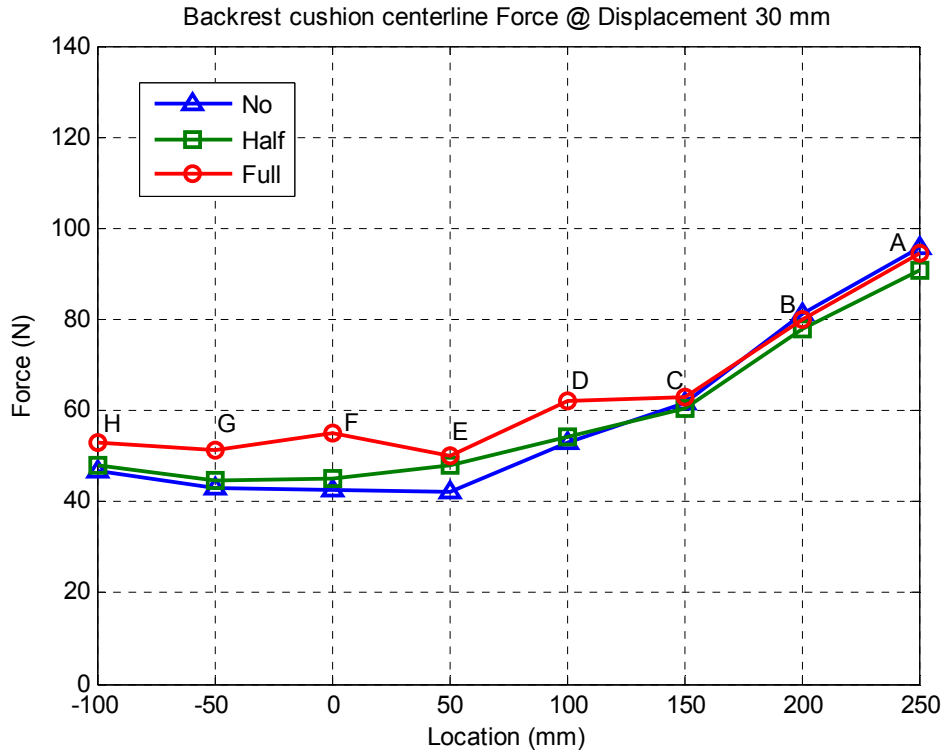

Figure 6 Loading forces distributed along the centreline of the backrest with 30 mm deformation

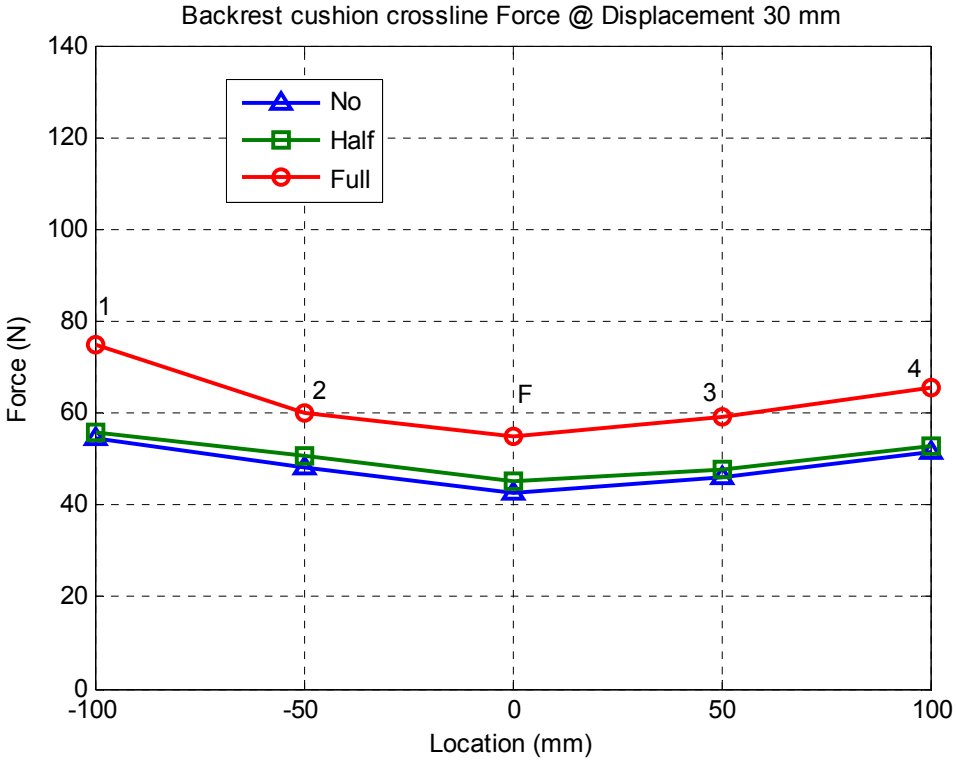

Figure 7 Loading forces distributed along the crossline of the backrest with 30 mm deformation

3.2 Seat transmissibilities in fore-and-aft direction

3.2.1 From the seat base to the backrest

The median transmissibilities of the eight subjects from the fore-and-aft acceleration at the seat base to the fore-and-aft acceleration at the backrest, tested with three magnitudes of random excitations and three extra lumbar support conditions are shown in Figure 8. A clear first resonance was observed in the frequency range of 3 – 4.5 Hz. With the lumbar support changed from "No" to "Half" and to "Full" positions, the transmissibility at the resonance frequency decreased for all three vibration magnitudes (p<0.013, Friedman). The resonance frequency increased slightly (0.25 ms^{-2} r.m.s.: p<0.037, Friedman) with increasing the lumbar support, but no evident change of the resonance frequency was found at the vibration magnitudes of 0.5 and 1.0 ms^{-2} r.m.s. (p>0.05, Friedman).

The median and individual fore-and-aft transmissibilities from the seat base to the backrest for the "No" lumbar support condition with three vibration magnitudes were shown in Figure 9. Both the resonance frequency (p<0.001, Friedman) and the transmissibility at the resonance (p<0.031, Friedman) decreased with increased vibration magnitude for the median and individual data of most subjects. Similar results were found for the other two lumbar support conditions.

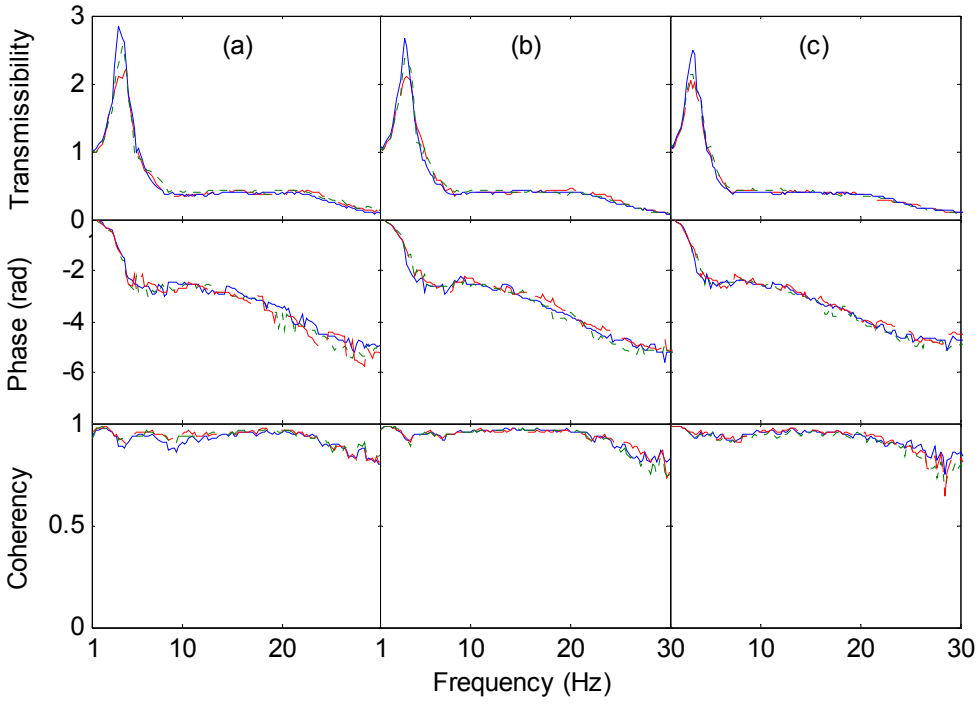

Figure 8 Median fore-and-aft transmissibility of 8 subjects from the seat base to the backrest in three magnitudes of excitations: (a) 0.25 ms^{-2} r.m.s., (b) 0.5 ms^{-2} r.m.s., (c) 1.0 ms^{-2} r.m.s. Lumbar support condition: — "No"; -·-·-, "Half"; – –, "Full".

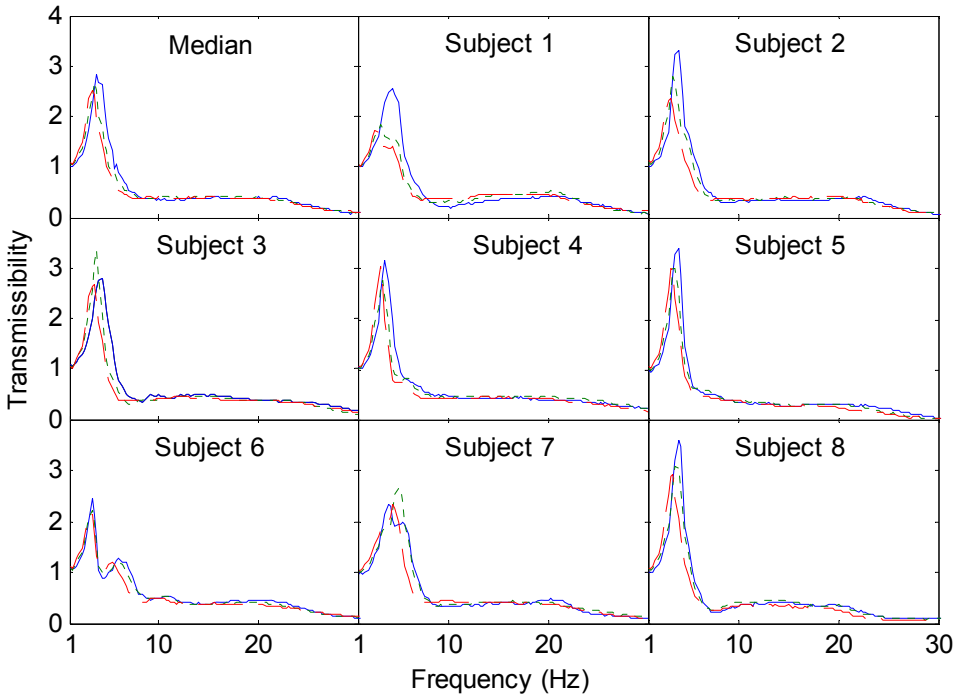

Figure 9 Median and individual fore-and-aft transmissibilities of 8 subjects from the seat base to the backrest in "No" lumbar support condition with three magnitudes of excitations: —, 0.25; -·-·- 0.5; – – 1.0 ms^{-2} r.m.s.

3.2.2 From the seat base to the seat pan

The median fore-and-aft transmissibility of the eight subjects from the seat base to the seat pan showed a clear first resonance in the frequency range of 3 – 4 Hz and a second resonance around 20 Hz for the three lumbar support conditions (Figure 10). With increasing the lumbar support from "No" to "Half" and to "Full" positions, the transmissibilities were increased at frequencies less than 8 Hz and decreased at a frequency range of 8 to 20 Hz. The transmissibilities at the primary resonance (p<0.05, Friedman) were increased with increasing the lumbar support. There is no obvious change in resonance frequency with changing the lumbar support conditions. Good coherencies were obtained in the transmissibilities from the seat base to the seat pan.

With increasing the magnitude of fore-and-aft vibration, the resonance frequencies of the transmissibility from the seat base to the seat pan shifted to the left for both the median and individual transmissibilites of most subjects (Figure 11 for "No" lumbar support condition). The reduction of the primary resonance frequency with increasing the vibration magnitude is significant for ''No'' lumbar support condition (p<0.01, Friedman). The change of the transmissibility at the resonance with the vibration magnitude was not as apparent as the change of the resonance frequency. Similar results were found for the other two lumbar support conditions.

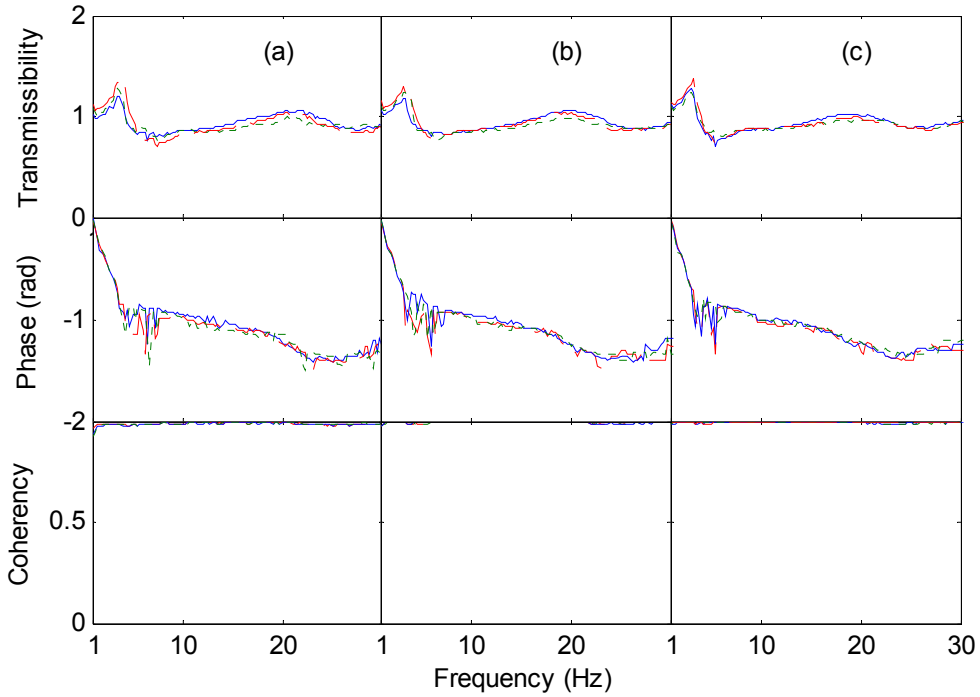

Figure 10 Median fore-and-aft transmissibility of 8 subjects from the seat base to the seat pan in three magnitudes of excitation: (a) 0.25 ms^{-2} r.m.s., (b) 0.5 ms^{-2} r.m.s., (c) 1.0 ms^{-2} r.m.s. Lumbar support condition: — "No"; -·-·-, "Half"; – –, "Full".

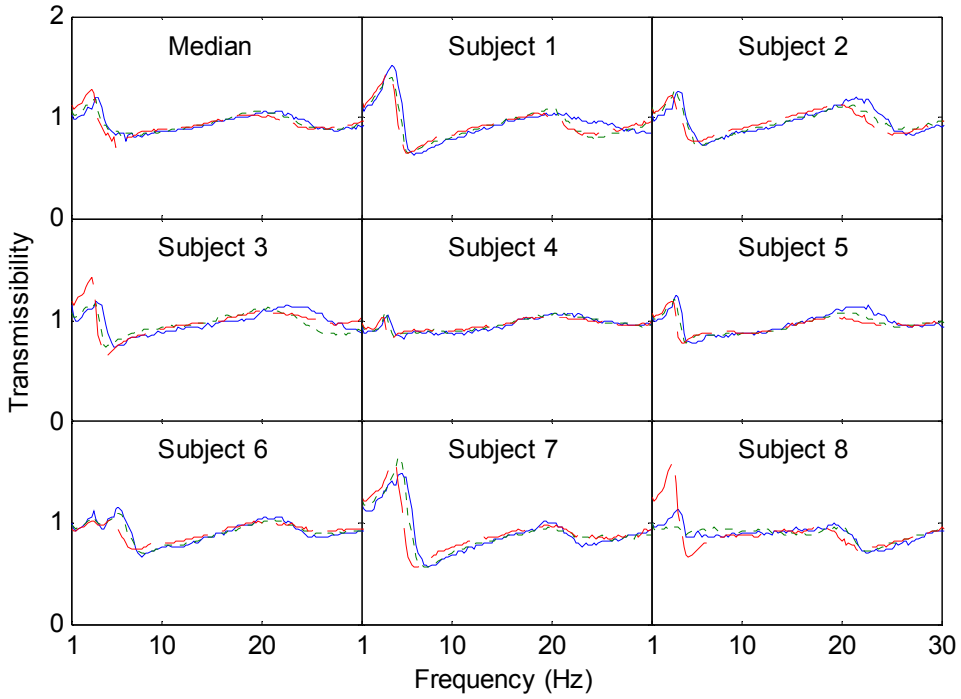

Figure 11 Median and individual fore-and-aft transmissibilities of 8 subjects from the seat base to the seat pan in "No" lumbar support condition exposed to three magnitudes of excitations: —, 0.25; -·-· 0.5; – – 1.0 ms^{-2} r.m.s.

4. Discussion

The extra lumbar support of the backrest affected both the static performance and vibration transmission of the car seat. The effect of lumbar support on hardness distribution of the backrest was mainly concentrated on the lumbar area in the vicinity of the adjustable lumbar support. The backrest of the test seat was a shaped foam embedded between the fabric cover and the meshed stainless structure with four springs connecting to the backrest frame. When rotating the lumbar support knob clockwise, the meshed structure became more bent so as to give an extra pushing force as if a preload was applied on to the foam. The foam in the lumbar contact area was subsequently pushed towards the back of the subject to give the lumbar an extra support. As a result, the backrest cushion became stiffer with increasing the lumbar support (Figure 5) and to some extent may increase the static comfort of the car seat as the pressure at the lower back of the seated human was enhanced (Kyung and Nussbaum, 2008). This is consistent with the result that dynamic stiffness of a foam cushion increases with increasing the preload or decreasing the thickness of foam (Zhang *et al.*, 2013). For the consideration of static comfort, it has been suggested that the apex of the lumbar contour should be positioned between 105 and 150 mm above the H-point so as to capture the lumbar area for most of the people (Reed *et al*, 1995; Reed and Schneider, 1996).

The increase in the extra lumbar support from “No” to “Half” and to “Full” positions did not produce a linear increase in the loading force when the same displacement was applied, indicating that the static stiffness was nonlinear with the change of the lumbar support conditions, as shown in Figures 6 and 7. This may be due to the nonlinear characteristic exhibited in the combined meshed stainless structure and the shaped foam. This phenomenon should be taken into consideration when modelling the seat-human system. It was also found that when the lumbar support was increased to the “Full” position, the loading force at point 1 was slightly higher than its mirrored point along the crossline of the backrest (Figure 7), showing that the extra lumbar support structure of the test seat is not symmetric. This may lead to non-uniformly distributed pressure in the lumbar region and cause premature fatigue and low back pain to the driver and passengers.

With increasing the lumbar support, the transmissibility (from the seat base to the backrest) at the resonance was found to decrease. This may be because the extra lumbar support stabilised the upper body movement and reduced the pelvis rotation, especially at the resonance frequency. The increase of the lumbar support may push the back of the body slightly forward, to some extent equivalent to reducing the inclination angle of the backrest. A previous study found that both the resonance and the peak at the resonance of the fore-and-aft transmissibility to the backrest of a car seat decreased when the backrest inclination decreased (Jalil and Griffin, 2007b). Indeed, a change of lumbar support condition may also cause some posture change of the subject. Subjects would experience involuntary posture change from a relatively “slouched” posture to a more “erect” posture when the lumbar support was changed from “No” to “Full” condition, which can cause changes of the mass distribution at the seat pan and the backrest and further affect the vibration transmission to these locations. The transmissibility from the seat base to the seat pan at the primary resonance was however, found to slightly increase when increasing the lumbar support. This may imply that the changes of the lumbar support have less

effect on the vibration transmission to the seat pan than to the backrest in the fore-and-aft direction. Further studies may be needed in order to confirm whether this is true and how this can be caused.

Consistent with previous studies (Qiu and Griffin, 2003; Jalil and Griffin, 2007b; Zhang *et al*., 2015), the decreased resonance frequency and the associated peak in the transmissibility from the seat base to the backrest with increasing the vibration magnitude in the three lumbar support conditions indicated a softening effect of the seated human body-seat system. The results might be due to the changes of the dynamic stiffness of the backrest cushion and biodynamics of the seated human body because of changing posture. It has been reported that the dynamic stiffness of foam seat was decreased with increasing vibration magnitude (e.g. Wei and Griffin, 1998; Zhang, 2013), and the resonance frequency of the fore-and-aft apparent mass at the backrest tested with subjects sitting on rigid seats shifted to the lower frequency range when increasing the magnitudes of fore-and-aft whole-body vibration (e.g. Fairley and Griffin, 1990; Nawayseh and Griffin, 2005, Qiu and Griffin, 2010, Qiu and Griffin, 2012).

5. Conclusion

This study aimed at investigating the effect of lumbar support on static seat performance and the fore-and-aft vibration transmission through the seat. It was found significant changes of seat hardness distribution in the main lumbar support area when changing the lumbar support conditions. The vibration transmission through the seat showed consistent changes when adjusting the lumbar support, especially for the resonance and the associated transmissibilities from the seat base to the backrest. The softening effect was also evident with increasing vibration magnitudes, indicating the non-linearities of the seat and human coupling system. It is anticipated the lumbar support may affect the ride comfort.

Acknowledgements

This research was funded by China Automotive Technology and Research Centre (CATARC).

Reference

Andersson BJG, Örtengren R, Nachemason A and Elfström G (1974) Lumbar disc pressure and myoelectric back muscle activity during sitting. iv. studies on a car driver's seat. Scandinavian Journal of Rehabilitation Medicine, 6 (3),128–133.

British Standards Institution (1987) Measurement and evaluation of human exposure to whole-body mechanical vibration and repeated shock. British Standard, BS 6841.

DeShaw J, Rahmatalla S (2014) Predictive discomfort in single- and combined-axis whole-body vibration considering different seated postures. Human Factors, 56 (5), 850-863.

Ebe K and Griffin MJ (2000) Qualitative models of seat discomfort including static and dynamic factors. Ergonomics 43 (6), 771–790.

Ebe K and Griffin MJ (2001) Factors affecting static seat cushion comfort. Ergonomics 44, 901–921.

Fairley TE and Griffin MJ (1990) Apparent mass of the seated human body in the fore-and-aft and lateral directions. Journal of Sound and Vibration, 139 (2), 299-306.

International Organization for Standardization (1992) Mechanical vibration Laboratory method for evaluating vehicle seat vibration - Part 1: Basic requirements, International Standard, ISO 10326-1.

International Organization for Standardization (1997) Mechanical vibration and shock - evaluation of human exposure to whole-body vibration - Part 1: General requirements, International Standard, ISO 2631-1.

Jalil NAA and Griffin MJ (2007a) Fore-and-aft transmissibility of backrests: Variation with height above the seat pan and non-linearity. Journal of Sound and Vibration 299 (1-2), 109-122.

Jalil NAA and Griffin MJ (2007b) Fore–and–aft transmissibility of backrests: Effect of backrest inclination, seat–pan inclination, and measurement location. Journal of Sound and Vibration 299 (1-2), 99–108.

Kamijo Km Tsujimura H, Obara H and Katsumata M (1982) Evaluation of seating comfort. SAE technical paper. No. 820761.

Kolich M (2003) Automobile seat comfort: Occupant preferences vs. anthropometric accommodation. Applied Ergonomics, 34 (2), 177-184.

Kyung G and Nussbaum MA (2008) Driver sitting comfort and discomfort (part II): Relationships with and prediction from interface pressure. International Journal of Industrial Ergonomics, 38 (5-6), 526-538.

Matsumoto Y, Ohdo K and Saito T (2006) Dynamic and subjective responses of seated subjects exposed to simultaneous vertical and fore-and-aft whole-body vibration: The effect of the phase between the two single-axis components. Journal of Sound and Vibration, 298 (3), 773 – 787.

Nawayseh N and Griffin MJ (2005) Non–linear dual–axis biodynamic response to fore–and–aft whole–body vibration. Journal of Sound and Vibration 282 (3–5), 831–862.

Qiu Y and Griffin MJ (2003) Transmission of fore-aft vibration to a car seat using field tests and laboratory simulation. Journal of Sound and Vibration 264 (1), 135-155.

Qiu Y and Griffin MJ (2010) Biodynamic Response of the Seated Human Body to Single-axis and Dual-axis Vibration: Effect of Backrest and Non-linearity. Industrial Health, 48 (5), 615-627.

Qiu Y and Griffin MJ (2012) Biodynamic Responses of the Seated Human Body to Single-axis and Dual-axis Vibration. Industrial Health, 50 (1), 37-51.

Reed MP, Schneider LW and Eby BA (1995) Some effects of lumbar support contour on driver seated posture. SAE Technical Paper. No.950141. Society of Automotive Engineers, Inc., Warrendale,PA, USA.

Reed MP and Schneider LW (1996) Lumbar support in auto seats: conclusions from a study of preferred driving posture. SAE Technical Paper. No.960478. Society of Automotive Engineers, Inc.,Warrendale, PA, USA.

Viswanathan M, Jorgensen MJ, Kittusamy NK (2006) Field evaluation of a continuous passive lumbar motion system among operators of earthmoving equipment. International Journal of Industrial Ergonomics, 36 (7), 651-659.

Wei L and Griffin MJ (1998) The prediction of seat transmissibility from measrues of seat impedance. Journal of Sound and Vibration 214 (1), 121-137.

Zhang XL, Qiu Y and Griffin MJ (2013) Static and dynamic stiffness of the cushion of a car seat. Presented at the 48th United Kingdom Conference on the Human Response to Vibration, held at Sunningdale Park, Ascot, England, 16-18th September 2013.

Zhang XL, Qiu Y and Griffin MJ (2015) Transmission of fore-and-aft vibration to the seat pan, the backrest and the headrest of a car seat. Proceedings of the Institution of Mechanical Engineers, Part D: Journal of Automobile Engineering, 230 (6), 736-744.